Journal of Alloys and Compounds 588 (2014) 46–48

Contents lists available at ScienceDirect

Journal of Alloys and Compounds

journal homepage: www.elsevier.com/locate/jalcom

Magnetocaloric effect and martensitic transition in $Ni_{50}Mn_{36-x}Co_xSn_{14}$

L.H. Yang [a,b], H. Zhang [c], F.X. Hu [b], J.R. Sun [b], L.Q. Pan [a], B.G. Shen [b,*]

[a] Department of Physics, University of Science and Technology Beijing, Beijing 100083, PR China
[b] State Key Laboratory for Magnetism, Institute of Physics, Chinese Academy of Sciences, Beijing 100190, PR China
[c] School of Materials Science and Engineering, University of Science and Technology Beijing, Beijing 100083, PR China

ARTICLE INFO

Article history:
Received 9 October 2013
Accepted 26 October 2013
Available online 2 November 2013

Keywords:
Ni–Mn–Co–Sn
Martensitic transition
Magnetocaloric effect

ABSTRACT

The structural, magnetic and martensitic transition properties are systematically investigated for $Ni_{50}Mn_{36-x}Co_xSn_{14}$ (x = 0, 1, 2, and 3) alloys. X-ray diffraction reveals that all the compounds are in the cubic phase with the $L2_1$-type Heusler structure at room temperature. Temperature dependent magnetization indicates that the Curie temperatures of austenitic phases are almost unchanged with the substitution of Co for Mn. However, the martensitic transition temperatures firstly increase and then decrease with Co content increasing, which is different from the general dependency on the value of valence electrons per atom (e/a). The reason could be that the main driving force of martensitic transition for $Ni_{50}Mn_{36-x}Co_xSn_{14}$ is the hybridization between Ni and excess Mn rather than the value of e/a. Due to the strong coupling between magnetism and structure, $Ni_{50}Mn_{34}Co_2Sn_{14}$ exhibits a large magnetocaloric effect, thereby making it a good candidate for magnetic refrigeration materials.

1. Introduction

The magnetocaloric effect (MCE) is the thermodynamic phenomenon of a magnetic material, which is subjected to the variation of magnetic field. Magnetic refrigeration based on MCE is considered to be environmental friendly and energy efficient compared with conventional gas-compression refrigeration. Over the past few years, magnetocaloric materials have been investigated extensively, and so far, a great number of magnetocaloric materials with giant MCE have been found, such as $Gd_5Si_2Ge_2$ [1,2], La(Fe, Si)$_{13}$ [3–5], $MnAs_{1-x}Sb_x$ [6], $MnFeP_{1-x}As_x$ [7], and Ni–Mn–X (X = Ga, In, Sn, etc.) Heusler alloys [8–10]. Due to the low cost of raw materials, non-toxic elements, and the tunableness of martensitic transition temperatures (T_M), Heusler alloys are particularly attractive as magnetic refrigeration materials.

In stoichiometric Ni_2MnSn alloy, no martensitic transition is observed. However, Mn-rich $Ni_{50}Mn_{25+x}Sn_{25-x}$ compounds, in which the excess Mn atoms occupy the vacant Sn (4b) sites, exhibit the martensitic transition from high-symmetry austenitic phase to a low symmetry martensitic phase [11]. The $Ni_{50}Mn_{36}Sn_{14}$ alloy undergoes a martensitic transition around 240 K from austenite phase with $L2_1$-type Heusler structure to martensitic phase with orthorhombic four-layered structure. Meanwhile, the $Ni_{50}Mn_{36}Sn_{14}$ alloy also exhibits an incipient antiferromagnetic ordering between Mn atoms located at Sn (4b) sites [12]. In order to elevate T_M and enhance saturation magnetization of austenite, we substitute Co atoms for Mn in $Ni_{50}Mn_{36}Sn_{14}$ alloy. By investigating martensitic transition properties of $Ni_{50}Mn_{36-x}Co_xSn_{14}$, we obtain some unusual results, in which the general law of the linear dependence of T_M on e/a loses effectiveness.

2. Experimental details

Polycrystalline specimens of $Ni_{50}Mn_{36-x}Co_xSn_{14}$ (x = 0, 1, 2, and 3) were prepared by arc melting an appropriate quantity of high-purity elements in argon atmosphere. The alloys were annealed at 1173 K for 96 h for further homogenization. The phase and crystal structure were examined by an X-ray powder diffractometer (XRD) equipped with Cu Kα (λ = 1.5406 Å) radiation. The isothermal and isofield magnetic properties were measured in an MPMS SQUID VSM magnetometer from Quantum Design Inc.

3. Results and discussion

Fig. 1 shows the room-temperature X-ray diffraction (XRD) patterns of $Ni_{50}Mn_{36-x}Co_xSn_{14}$ (x = 0, 1, 2, and 3) alloys. It is observed that all the alloys have a pure cubic austenitic structure, indicating that T_M are below room temperature. The super lattice reflections (the Miller indices h, k, l are all odd) such as (1 1 1) and (3 1 1) are observed, implying the highly ordered $L2_1$ phase [13].

Thermomagnetic curves are measured in order to study the phase transition characteristics of $Ni_{50}Mn_{36-x}Co_xSn_{14}$ compounds. Fig. 2(a) shows the temperature dependences of zero-field-cooled (ZFC) and field-cooled (FC) magnetization in a magnetic field of 0.01 T for $Ni_{50}Mn_{34}Co_2Sn_{14}$ alloy. Three phase transitions are observed with the variation of temperature. In the temperature range of above 283 K, a magnetic transition from ferromagnetic

* Corresponding author. Tel.: +86 1082648082.
E-mail address: shenbg@aphy.iphy.ac.cn (B.G. Shen).

0925-8388/$ - see front matter © 2013 Elsevier B.V. All rights reserved.
http://dx.doi.org/10.1016/j.jallcom.2013.10.196

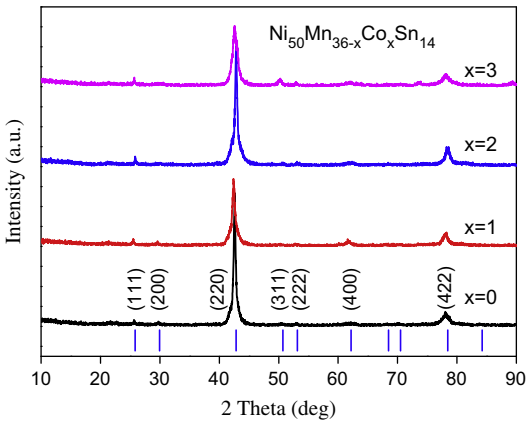

Fig. 1. The XRD patterns of $Ni_{50}Mn_{36-x}Co_xSn_{14}$ (x = 0, 1, 2, and 3) alloys at room temperature.

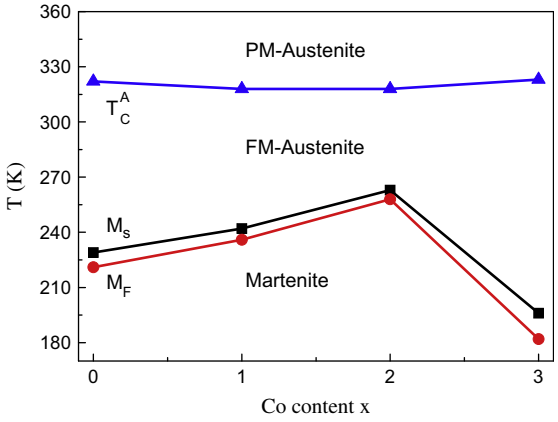

Fig. 3. Phase diagram of $Ni_{50}Mn_{36-x}Co_xSn_{14}$ (x = 0, 1, 2, and 3) compounds.

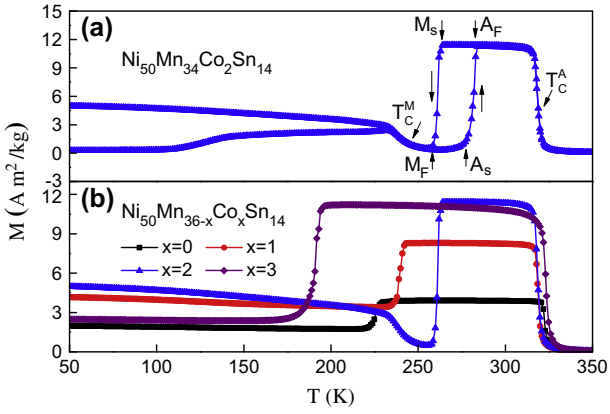

Fig. 2. (a) Temperature dependences of ZFC and FC magnetization in a magnetic field of 0.01 T for $Ni_{50}Mn_{34}Co_2Sn_{14}$ and (b) temperature dependences of FC magnetization in 0.01 T for $Ni_{50}Mn_{36-x}Co_xSn_{14}$ (x = 0, 1, 2, and 3).

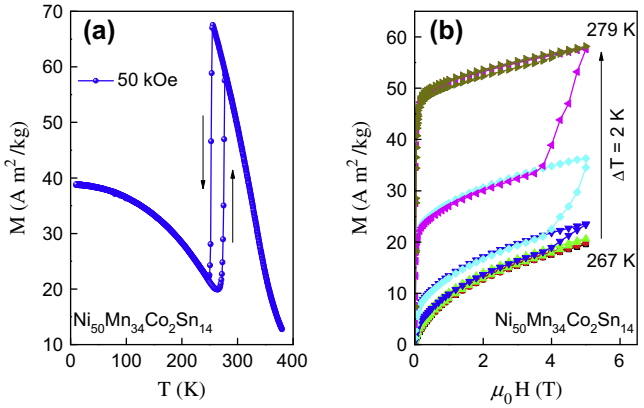

Fig. 4. (a) Temperature dependences of ZFC and FC magnetization in a magnetic field of 5 T for $Ni_{50}Mn_{34}Co_2Sn_{14}$ and (b) isothermal magnetization curves for $Ni_{50}Mn_{34}Co_2Sn_{14}$ in the vicinity of the martensitic transition.

(FM) austenite to paramagnetic (PM) austenite is observed around the Curie temperature $T_C^A \approx 318$ K. In the temperature range of 257–283 K, martensitic and inverse martensitic phase transitions can be found to occur at characteristic temperatures of martensite-start temperature (M_S) of 264 K, martensite-finish temperature (M_F) of 257 K, austenite-start temperature (A_S) of 275 K, and austenite-finish temperature (A_F) of 283 K. As a typical characteristic of first order phase transition, a large hysteresis between martensitic and inverse martensitic transitions is observed. In the temperature range of below 257 K, the other magnetic phase transition from FM martensite to PM martensite is observed around the Curie temperature $T_C^M \approx 238$ K. With temperature further decreasing, a splitting between ZFC and FC is observed, which may be due to magnetical inhomogeneity [14,15]. Fig. 2(b) presents temperature dependences of FC magnetization in 0.01 T for $Ni_{50}Mn_{36-x}Co_xSn_{14}$ (x = 0, 1, 2, and 3) alloys. Martensitic transition can be seen clearly in all the compounds. Especially, $Ni_{50}Mn_{34}Co_2Sn_{14}$ experiences the martensitic transition from FM austenitic phase of high magnetization to PM martensitic phase of low magnetization, leading to a large magnetization difference ΔM. This result is attributed to the fact that the value of T_C^M is lower than that of M_F.

Fig. 3 shows the phase diagram of $Ni_{50}Mn_{36-x}Co_xSn_{14}$ (x = 0, 1, 2, and 3) alloys with temperature increasing. The characteristic temperatures of phase transitions (M_S, M_F, and T_C^A) are determined from Fig. 2(b). It is observed that the values of T_C^A remain nearly constant with the substitution of Co for Mn. However, the values of M_S and M_F firstly increase with Co content increasing from x = 0 to x = 2, and then decrease with Co content further increasing to x = 3. It has been reported that the T_M increases generally with the value of e/a in NiMn-based Heusler alloys [11,16]. For $Ni_{50}Mn_{36-x}Co_xSn_{14}$ alloys, the valence electrons are defined as the number of 3d and 4s electrons of Ni, Mn and Co, and the number of 5s and 5p electrons of Sn. The obtained values of e/a in $Ni_{50}Mn_{36-x}Co_xSn_{14}$ increase monotonically with Co content, while the values of T_M does not increase monotonically with Co content. Similar phenomena have been observed in other Heusler alloys, such as $Ni_{50}(Mn_{1-x}Fe_x)_{36}Sn_{14}$ [17], $Ni_{50}Mn_{35-x}Cu_xSn_{15}$ [18], $Ni_{50}Mn_{38-x}Fe_xSb_{12}$ [19]. Ye et al. [20] and Khan et al. [21] studied the underlying mechanism of martensitic transition, and gave the conclusion that the hybridization between Ni 3d e_g states and the 3d states of excess Mn atoms at Sn sites was the main driving force for Mn-rich Heusler alloys. In this situation, once the hybridization is established, any change in the Ni or Mn content would tend to weaken the hybridization and reduce T_M. For $Ni_{50}Mn_{36-x}Co_xSn_{14}$ alloys, T_M at first increases with the Co content for complicated factors, such as crystallographic symmetry [22], and the change of Fermi surface and the Brillouin zone boundary [23]. However, T_M eventually decreases with further increasing Co content for the weakened hybridization which is the dominant factor now.

A large ΔM across the martensitic transition predicts a large Zeeman energy $\mu_0 \Delta M \cdot H$ and thus a field-induced structural transformation [24]. Fig. 4(a) exhibits the temperature dependences of ZFC and FC magnetization in a magnetic field of 50 kOe for $Ni_{50}Mn_{34}Co_2Sn_{14}$ alloy. Due to the large ΔM of 44 emu/g obtained

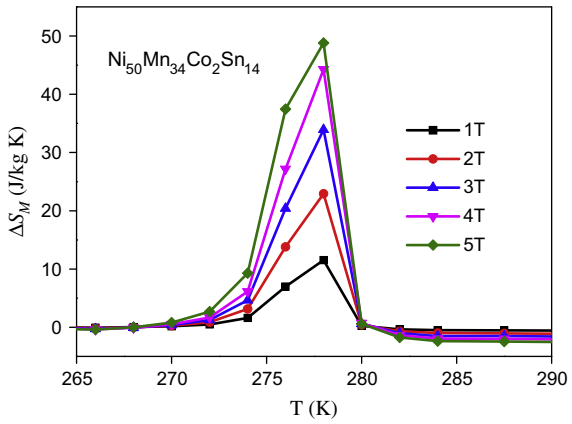

Fig. 5. Magnetic entropy changes for $Ni_{50}Mn_{34}Co_2Sn_{14}$ alloy in 1, 2, 3, 4 and 5 T magnetic fields, respectively.

from Fig. 4(a) and the high M_S of 259 K, the $Ni_{50}Mn_{34}Co_2Sn_{14}$ alloy is chosen to measure isothermal magnetization curves and to evaluate MCE from the practical angle. Fig. 4(b) shows the isothermal magnetization curves of $Ni_{50}Mn_{34}Co_2Sn_{14}$ in the vicinity of martensitic transition during increasing temperature in temperature steps of 2 K. One can observe a large magnetic hysteresis, which is a signature of first-order phase transition. The compound exhibits paramagnetism below 267 K, while it shows strong FM coupling above 279 K. In the temperature range from 267 to 279 K, the magnetization shows a sharp rise around 3.8 T, indicating the field-induced metamagnetic transition from weak magnetic martensite to strong magnetic austenite.

The magnetic entropy change (ΔS_M) in the vicinity of martensitic transition is calculated from the isothermal magnetization curves by using the Maxwell relation $\Delta S_M = \int_0^H (\partial M/\partial T)_H dH$. The temperature dependences of ΔS_M under different fields for $Ni_{50}Mn_{34}Co_2Sn_{14}$ alloy are presented in Fig. 5. The observed positive ΔS_M value represents the inverse MCE. Due to field-induced metamagnetic transition from low magnetic martensite to high magnetic austenite, the peaks of ΔS_M broaden toward lower temperature. For the strong coupling between the magnetism and structure, the maximal values of ΔS_M reach 22.9 J kg^{-1} K^{-1} and 48.8 J kg^{-1} K^{-1} for a field change of 0–2 T and 0–5 T, respectively. Such a large MEC comparable to those of $Ni_{44}Mn_{43}Cu_2Sn_{11}$ [24] and $Ni_{43}Mn_{43}Co_4Sn_{11}$ [25], makes $Ni_{50}Mn_{34}Co_2Sn_{14}$ a good candidate for magnetic refrigeration materials.

4. Conclusions

In this paper, we investigate the effects of substituting Mn with Co on structural, magnetic, and martensitic transition properties in $Ni_{50}Mn_{36}Sn_{14}$ alloy. The substitution can hardly move the Curie temperature in austenitic phase, but shift martensitic transition temperature clearly. With the increase of Co content, martensitic transition temperature first increases and then decreases, which is likely to be caused by the hybridization between Ni 3*d* e_g states and the 3*d* states of excess Mn. Due to the strong coupling between magnetic and structural phase transitions, $Ni_{50}Mn_{34}Co_2Sn_{14}$ exhibits a large MEC of ΔS_M = 22.9 J kg^{-1} K^{-1} for a magnetic field change of 2 T, thereby making it a potential candidate for magnetic refrigeration materials.

Acknowledgements

This work was supported by the National Natural Science Foundation of China, the Hi-Tech Research and Development program of China, the Key Research Program of the Chinese Academy of Sciences, and the National Basic Research of China.

References

[1] V.K. Pecharsky, K.A. Gschneidner Jr., Phys. Rev. Lett. 78 (1997) 4494.
[2] K.A. Gschneidner Jr., V.K. Pecharsky, A.O. Tsokol, Rep. Prog. Phys. 68 (2005) 1479.
[3] F.X. Hu, B.G. Shen, J.R. Sun, X.X. Zhang, Chin. Phys. 9 (2000) 550.
[4] F.X. Hu, B.G. Shen, J.R. Sun, Z.H. Chen, G.H. Rao, X.X. Zhang, Appl. Phys. Lett. 78 (2001) 3675.
[5] B.G. Shen, J.R. Sun, F.X. Hu, H.W. Zhang, Z.H. Chen, Adv. Mater. 21 (2009) 4545.
[6] H. Wada, Y. Tanabe, Appl. Phys. Lett. 79 (2001) 3302.
[7] O. Tegus, E. Brück, K.H.J. Buschow, F.R. de Boerm, Nature (London) 415 (2002) 150.
[8] F.X. Hu, B.G. Shen, J.R. Sun, Appl. Phys. Lett. 76 (2000) 3460.
[9] T. Krenke, E. Duman, M. Acet, E.F. Wassermann, X. Moya, L. Mañosa, A. Planes, Nat. Mater. 4 (2005) 450.
[10] J. Liu, T. Gottschall, K.P. Skokov, J.D. Moore, O. Gutfleisch, Nat. Mater. 11 (2012) 620.
[11] T. Krenke, M. Acet, E.F. Wassermann, X. Moya, L. Mañosa, A. Planes, Phys. Rev. B 72 (2005) 014412.
[12] P.J. Brown, A.P. Gandy, K. Ishida, R. Kainuma, T. Kanomata, K-U Neumann, K. Oikawa, B. Ouladdiaf, K.R.A. Ziebeck, J. Phys.: Appl. Phys. 18 (2006) 2249.
[13] S.E. Muthu, N.V.R. Rao, M.M. Raja, D.M.R. Kumar, D.M. Radheep, S. Arumugam, J. Phys. D: Appl. Phys. 43 (2010) 425002.
[14] B. Gao, F.X. Hu, J. Shen, J. Wang, J.R. Sun, B.G. Shen, J. Magn. Magn. Mater. 321 (2009) 2571.
[15] C. Jing, Z. Li, H.L. Zhang, J.P. Chen, Y.F. Qiao, S.X. Cao, J.C. Zhang, Eur. Phys. J. B 67 (2009) 193.
[16] T. Krenke, M. Acet, E.F. Wassermann, X. Moya, L. Mañosa, A. Planes, Phys. Rev. B 73 (2006) 174413.
[17] E.C. Passamani, F. Xavier, E. Favre-Nicolin, C. Larica, A.Y. Takeuchi, I.L. Castro, J.R. Proveti, J. Appl. Phys. 105 (2009) 033919.
[18] B. Gao, J. Shen, F.X. Hu, J. Wang, J.R. Sun, B.G. Shen, Appl. Phys. A 97 (2009) 443.
[19] R. Sahoo, A.K. Nayak, K.G. Suresh, A.K. Nigam, J. Appl. Phys. 109 (2011) 123904.
[20] M. Ye, A. Kimura, Y. Miura, M. Shirai, Y.T. Cui, K. Shimada, H. Namatame, M. Taniguchi, S. Ueda, K. Kobayashi, R. Kainuma, T. Shishido, K. Fukushima, T. Kanomata, Phys. Rev. Lett. 104 (2010) 17640.
[21] M. Khan, J. Jung, S.S. Stoyko, A. Mar, A. Quetz, T. Samanta, I. Dubenko, N. Ali, S. Stadler, K.H. Chow, Appl. Phys. Lett. 100 (2012) 172403.
[22] L. Ma, H.W. Zhang, S.Y. Yu, Z.Y. Zhu, J.L. Chen, G.H. Wu, H.Y. Liu, J.P. Qu, Y.X. Li, Appl. Phys. Lett. 92 (2008) 032509.
[23] P.J. Webster, K.R.A. Ziebeck, S.L. Town, M.S. Peak, Philos. Mag. B 49 (1984) 295.
[24] R. Das, S. Sarma, A. Perumal, A. Srinivasan, J. Appl. Phys. 109 (2011) 07A90.
[25] Z. Han, D. Wang, B. Qian, J. Feng, X. Jiang, Y. Du, Jpn. J. Appl. Phys. 49 (2010) 010211.